Unipolar arc model

Document Version:
Publisher's PDF, also known as Version of Record (includes final page, issue and volume numbers)

Please check the document version of this publication:

• A submitted manuscript is the version of the article upon submission and before peer-review. There can be important differences between the submitted version and the official published version of record. People interested in the research are advised to contact the author for the final version of the publication, or visit the DOI to the publisher's website.
• The final author version and the galley proof are versions of the publication after peer review.
• The final published version features the final layout of the paper including the volume, issue and page numbers.

Link to publication

Unipolar Arc Model

HERMAN J. G. GIELEN AND DANIEL C. SCHRAM

Abstract—A three-dimensional description of an axisymmetric unipolar arc discharge is given. Both sheath and plasma ball effects are taken into account. The analysis is based on the simultaneous solution of Ohm's law, Maxwell equations, and the boundary conditions for the electric potential at the plasma–sheath interface. These boundary conditions are dictated by the sheath effects. The potential distribution, current distribution, and magnetic fields in the plasma have been determined for a given electron density profile. These calculations show that the unipolar arc arises as a natural consequence of the pressure force.

Fig. 1. Unipolar arc model.

I. INTRODUCTION

THE OCCURRENCE of unipolar or plasma-induced arc discharges has been known since the late 1950's. Robson and Thoneman [1] were the first to describe these phenomena, and they introduced the term "unipolar arc." Essential for these kind of discharges is that one electrode serves both as cathode and anode—this in contrast to normal bipolar arcs. In fusion reactors the unipolar plasma–wall interaction produces high-Z impurities that cool the plasma [2]–[5]. Also, in laser-produced plasmas the effect of plasma-induced arcing, known as laser pitting, has been studied [6].

The basis for the Robson–Thoneman unipolar arc model is illustrated in Fig. 1. When no arcing occurs (Fig. 1(a)), the floating sheath potential V_f prevents all but the higher energy electrons in the Maxwellian distribution from reaching the surface. If V_f exceeds the potential to initiate and sustain an arc, then there will be a strong local emission of electrons from the cathode spot on the electrode into the plasma (Fig. 1(b)). In the vicinity of the spot the plasma potential will be lowered and more electrons can return to the electrode there. The return flow of electrons closes the current loop of the unipolar arc. In their original paper, Robson and Thoneman assumed a constant electron density and a constant reduction of the sheath potential over the whole plasma-wall boundary, contributing over a large area of the wall. However, the occurrence of the cathode spot implies an enhancement of the electron and ion density near the spot. This concept is incorporated in the model of Schwirkze [7], who gives an essentially qualitative description of the unipolar arc. In
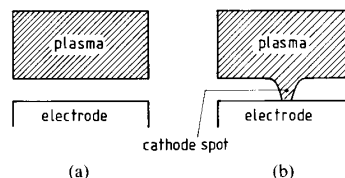
this model, the electric fields induced by the pressure gradient in the plasma above the sheath determine the characteristics of the discharge. Other models are given by [8]–[10]. The analysis given by Wieckert [8] does not take into account the effects of the plasma above the sheath. Ecker *et al.* [10] do incorporate to some extent these effects in their model. However, this model is essentially one-dimensional and no details of the current backflow can be derived from it. Ecker *et al.*'s calculation shows that the electromotive force induced in the plasma can be more important than the sheath-induced electromotive force. The discussion given by Hantzsche [9] extensively treats the sheath pheonomena.

In this paper we give a three-dimensional description of an axisymmetric arc in which both sheath and plasma phenomena are incorporated. The sheath phenomena are reflected in the boundary conditions for the plasma, similar to the approach of [8]. The basis for our model is the simultaneous solution of Ohm's law, Maxwell equations, and the boundary conditions. The model elaborates upon the electric, current density, and magnetic fields in the plasma ball above the sheath. Both pressure and magnetic effects are included. We will first discuss the sheath phenomena that will impose boundary conditions on the description of the plasma.

II. SHEATH PHENOMENA

As we will discuss later, the solution of the electron momentum equation assumes an electron density and temperature profile in the region above the sheath. This density profile is given in Fig. 2. We follow [9] by assuming an electron density profile which can be considered as a superposition of two different plasmas: 1) A background plasma of relatively low electron density; and 2) a high-density cathode plasma at a temperature of a few eV.

When the electron temperature of the background plasma is high (>10 eV), the arc configuration as given in Fig. 2 resembles a plasma-induced arc in fusion devices. When, however, the background is at a temperature
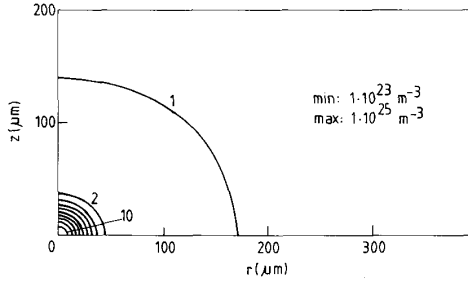
Fig. 2. The assumed electron density profile. Numbers indicate different contour levels.

comparable to the value in the cathode spot, the discharge resembles a vacuum arc. The description of both these plasmas is analogous [11]. They differ in background plasma, but the effects associated with the cathode spot are similar. The differences in background plasma cause the extension of the current backflow region to be different. For the vacuum arc, the constant background density can be regarded as an approximation of an essentially broader density profile superimposed upon the density profile describing the cathode spot. Due to this approximation the physical fields far from the spot will need a slight modification when an accurate description is needed there. The approximation will, however, not essentially influence the physics of the region near the spot that has our primary interest.

Here we will consider an isothermal plasma: Both the background and cathode plasma have the same electron temperature (3 eV). We assume that the sheath thickness, which is of the order of the Debye length, is small compared to the characteristic scale length of the cathode spot. Therefore we can incorporate in the description of the plasma above the sheath the sheath phenomena in the boundary conditions for the electric potential. To show this we first consider the current density dependence on the sheath potential, given by [1]

$$ j_\perp = \frac{1}{4} n_e e \sqrt{8kT_e/\pi m_e} \left\{ \exp\left(\frac{-eV_s}{kT_e}\right) - \exp\left(\frac{-eV_f}{kT_e}\right) \right\}. $$

$$ (1) $$

Here V_s is the potential difference between the sheath edge and wall, $\perp$ means perpendicular to the wall surface, and n_e is the electron density at the plasma–sheath interface. All voltages are given with respect to the wall. V_f is the floating potential given by

$$ V_f = (kT_e/2e) \ln (m_+/2\pi m_e) \qquad (2) $$

where T_e is the electron temperature, m_+ is the ion mass, and m_e is the electron mass. When the sheath edge is at this floating potential, there is no net current towards the electrode.

From (1) it is possible to calculate the sheath potential V_s for a given perpendicular component of the current density. At the cathode spot, however, the voltage drop

over the sheath equals the cathode fall. For copper, the cathode fall V_c is of the order of 15 V [12]. The cathode fall is nearly independent of the current [12]. Therefore, the fall is kept constant in our calculations; i.e., we do not assume any dependency on the current density. The cathode fall occurs within the crater of the spot. Equation (1) describes the current–voltage relation for the sheath. This current density has a minimum value $j_{\text{sheath-min}}$ for which all of the current is carried by the ions and all the electrons are inhibited to cross the sheath due to the high sheath potential. The quantity $j_{\text{sheath-min}}$ is given by

$$ j_{\text{sheath-min}} = -n_e e \sqrt{kT_e/m_+}. \qquad (3) $$

If the actual current density is less than this minimum current, we have to assume that arcing occurs there and that the sheath potential equals the cathode fall. In the iterative procedure described in the next section, used to solve the electron momentum equation, the sheath potential can be varied depending on the perpendicular component of the current density. This will be discussed further in the next section, where the plasma above the sheath is considered.

III. PLASMA PHENOMENA

Here we will consider the plasma above the sheath. The model described is a two-fluid model. We consider a plasma in which only singly ionized atoms play a role. The extension to a plasma in which also higher ionized atoms occur does not alter quantitatively the basic physical processes we want to describe here. We will assume that the degree of ionization is high enough to neglect the electron-neutral friction in the electron momentum equation. The model can be applied to axisymmetric plasmas. For the electromagnetic fields, we will assume that displacement currents can be neglected; i.e., that the quasi-static approximation can be applied. Furthermore, we will assume that the plasma can be considered static; i.e., that the relevant time scales are long enough to assure that the electric fields induced by a changing magnetic field are small compared to the electric fields induced by charges. Then the electric field can be derived from the electric potential φ_{el}.

Neglecting the inertia term, the electron momentum equation is given by

$$ \underline{0} = -\nabla p_e - en_e\underline{E} - en_e\underline{w}_e \times \underline{B} + en_e\eta\underline{j}. \qquad (4) $$

Here p_e is the electron pressure, $\underline{E}$ is the electric field, n_e is the electron density, $\underline{w}_e$ is the systematic electron velocity, $\underline{B}$ is the magnetic field, η is the resistivity, and $\underline{j}$ is the current density. Equation (4) is also referred to as Ohm's law. In most plasmas that have our interest, the current is carried almost completely by the electrons, implying that

$$ \underline{j} \approx -en_e\underline{w}_e. \qquad (5) $$

The current in the plasma ball of the cathode spot is carried for 80–90 percent by the electrons [13]. Therefore,

the motion of the ions has a small influence on the electromagnetic fields and is consequently neglected here.

For a quasi-static plasma $\nabla \cdot \underline{j} = 0$. Then condition (5) implies that the plasma is sourceless. With the simplification (5), we can, after division by en_e, write for the electron momentum equation:

$$0 = -\frac{1}{en_e} \nabla p_e - \underline{E} + \frac{(\underline{j} \times \underline{B})}{en_e} + \eta \underline{j}. \qquad (6)$$

As long as (5) is valid, the motion of the electrons is not directly influenced by the motion of the ions. As far as the electron dynamics are concerned, the whole of the physics of the interaction of electrons and ions is projected in the electric field and the resistivity η, which is temperature- and only weakly density-dependent. As the magnetic field is determined by the current density, the first, third, and the last terms in (6) are known for the given electron density and velocity of the isothermal electron gas. So the electric field can be expressed in "electron gas quantities," although its origin is found in the charge separation between electrons and ions. This implies that under the simplification (5) the current density and magnetic field, as well as the electric field, can be determined from the dynamics of the electron gas. This means, on the other hand, that the ion gas moves in electromagnetic force fields that are known for the given electron density and electron velocity.

This will be the basis for the model to be presented in the following. We shall calculate the electromagnetic quantities by solving the electron momentum equation. We will start from given density and temperature profiles for the electrons. In principle, both these quantities are measurable. We will use cylindrical coordinates (r, φ, z) throughout. Due to the axisymmetry, $\partial/\partial\varphi = 0$ for all physical scalar quantities. We want to stress that in general both $\underline{j}$ and $\underline{B}$ can have radial, azimuthal, and axial components. The radial and axial components together are called the meridional component. For example, the meridional current $\underline{j}_m$ density is given by

$$\underline{j}_m = j_r \underline{e}_r + j_z \underline{e}_z. \qquad (7)$$

The magnetic field can consist of two parts: It can be either sustained by external coils or can be a self-generated one due to electric currents in the plasma. So we can write,

$$\underline{B} = \underline{B}_{\text{applied}} + \underline{B}_{\text{generated}}. \qquad (8)$$

Rearranging (6) gives

$$\underline{E} = -\frac{1}{en_e} \nabla p_e + \frac{1}{en_e} \underline{j} \times \underline{B} + \eta \underline{j}. \qquad (9)$$

It is tempting to consider this equation as a generating equation for the electric field. However, (9) merely states the formal balance of forces acting on the electron gas and gives no information on the charge separation in the plasma that actually causes the generated electric field.

This charge separation can be determined from Coulomb's law:

$$\nabla \cdot \underline{E} = \rho/\epsilon_0. \qquad (10)$$

Here ϵ_0 is the permittivity. Neglecting the spatial dependence of the resistivity, the combination of (9) and (10) gives the charge separation in the plasma:

$$\rho = \epsilon_0 \nabla \cdot \left[-\frac{1}{en_e} \nabla p_e + \frac{1}{en_e} \underline{j} \times \underline{B} \right]. \qquad (11)$$

Through Poisson's equation this charge separation determines uniquely the electric potential φ_{el} once the boundary conditions are given. The boundary conditions on the electrode can be determined as given in the first section. These boundary conditions will depend on the current density $\underline{j}$. Equation (1) gives the relation between the sheath potential V_s and the normal component of the current density.

We can then calculate the quantity $\underline{g}$ defined by

$$\underline{g} := \frac{1}{\eta} \left[\frac{1}{en_e} \nabla p_e - \frac{1}{en_e} \underline{j} \times \underline{B} - \nabla \varphi_{el} \right]. \qquad (12)$$

This quantity has the dimension of a current density. For given electron density and electron temperature profiles and current density $\underline{j}$, the quantity $\underline{g}$ is determined uniquely, since the generated magnetic field can be determined from the current density through Ampère law. Referring to (9) we see, however, that if and only if $\underline{g} = \underline{j}$, these quantities describe a physically relevant plasma, satisfying Ohm's law, Maxwell equations, and the corresponding boundary conditions. Our aim is to find that current density $\underline{j}$ which, for the given electron density and temperature distribution, yields $\underline{g} = \underline{j}$. In the next section we will discuss an iterative procedure to determine this current density. A more extensive discussion of the solution strategy and several applications of this method to expanding plasmas is given by [14].

IV. ITERATIVE PROCEDURE

In this section we will describe an iterative procedure to solve the electron momentum equation. The basis for the iterative procedure used is the discussion in the last section. The electron density and temperature profiles are assumed to be known and do not change during iteration. For a current density distribution $\underline{j}$ we can calculate the generated magnetic field through Ampère law. This current density also determines the sheath potential which is used in the solution of Poisson's equation. Then it is possible to calculate, using (9)–(11), the charge separation, and through the Poisson equation, the electric potential φ_{el}. All the right-hand side (RHS) terms of (12) are known and the quantity $\underline{g}$ can be determined. When this quantity equals the current density $\underline{j}$, a solution of the electron momentum equation is obtained. If not, then the quantity $\underline{g}$ is taken to be the next approximation for the current density in the iterative scheme. This is repeated until convergence in $\underline{j}$ and $\underline{g}$ occurs. Then a solution is obtained sat-

isfying the electron momentum equation, Maxwell equations, and the sheath equation (1).

The iterative procedure is started with a current density equal to zero. Then only the pressure term has to be taken into consideration and the sheath potential equals the floating potential outside the crater of the spot.

V. RESULTS AND DISCUSSION

The electron momentum equation has been solved numerically using finite-element techniques on a VAX 8530 computer. Here we will give the results of these calculations.

When no external magnetic field is applied, the azimuthal component of $\underline{\mathfrak{J}}$ vanishes, as can be seen from the azimuthal component of (12):

$$\mathfrak{J}_\varphi \underline{e}_\varphi = \frac{-1}{e\eta n_e} \underline{j}_m \times \underline{B}_m. \qquad (13)$$

As the iterative calculation is started with $\underline{j} = \underline{0}$, both the azimuthal current density and the meridional magnetic field will remain zero throughout. When the iteration is started with a nonvanishing azimuthal current density, the converging solution also yields a vanishing one.

In the spot the gradient length for the electron density is much smaller than that for the electron temperature. Therefore we can, in evaluating the pressure term in the electron momentum equation, effectively assume a constant electron temperature.

For the calculations to be discussed we have assumed that $T_e = 3$ eV. Furthermore, a homogeneous resistivity ($\eta = 10^{-4}$ Vm/A) and a density profile n_e, as given in the contour plot in Fig. 2, are assumed. The density profile is presupposed; i.e., the electron density profile is not determined self-consistently from the model. The reason for assuming the electron density profile as given in Fig. 2 is that our aim is to describe an expanding plasma and to show that such a plasma induces an unipolar arc discharge. The assumed profiles are qualitatively what is to be expected from an expanding plasma driven by the pressure gradient in the plasma ball region of the spot. Changes in the parameters of the expansion do not qualitatively alter this conclusion.

The lines of constant electron density are ellipses in the r–z plane. The axial elongation of the electron density is 1.23 times the radial elongation. The contour lines are equally spaced between the minimum and maximum values of the electron density, given in the figure. As we assumed axisymmetry, all physical quantities can be represented in the two-dimensional r–z plane. Fig. 2 is an example of such a representation and shows the region for which the electron momentum equation has been solved. The region which we used for the calculations extends 1-mm radially and 0.2-mm axially. The large radial extension of the region is a consequence of the geometry of the current backflow to the electrode. The plane $z = 0$ is the cathode. The Poisson equation is solved on the region enclosing the whole of the plasma. Its boundary at the cath-

ode is formed by the edge of the sheath. At this edge the boundary conditions for the electric potential are derived from the axial component of the current density as given by (1). This is, of course, only possible for the region of the cathode where the current density exceeds the minimum current density $j_{sheath\text{-}min}$ as given in (3). When the axial current density is less than this minimum current density, the potential is taken to be the cathode fall. For numerical reasons, we asserted the simplification that the cathode fall equals the floating potential, and that $j_{sheath\text{-}min}$ equals zero. For a 3-eV Cu-plasma we find that $V_{float} = 14.75$ V. As this is of the same order as the cathode fall (15 V [12]), the first simplification is justified. The second simplification will be justified later. These simplifications assure that the potential distribution at the cathode rim is a smooth one. As no theoretical or experimental data are available on the potential distribution within the spot, the cathode fall is taken to be constant. To avoid discontinuities in the potential's derivative, corresponding to physically impossible infinite-charge densities, we assume a smooth transition of the potential over the crater rim. The occurrence of a potential hump at the crater edge cannot be excluded; certainly the mechanism of expelled metal fluid particles suggested by [15] could be an indication of such potential disturbances. In this first-order calculation we will ignore such a possible additional potential disturbance.

At the other boundaries we assume natural boundary conditions for the electric potential: $\partial\varphi_{el}/\partial n = 0$. At the left boundary, corresponding to the discharge axis, this is a direct consequence of the symmetry of the discharge. The upper and right boundaries are taken far from the spot, warranting a vanishing normal electric field there. For the numerical calculation the region was covered with a mesh of 1032 axisymmetric quadratic isoparametric triangles in R^3. The coarseness of the mesh increases from the cathode spot region where the gradient lengths are smallest.

For the assumed electron density and temperature profiles, the Lorentz term in the electron momentum equation is small compared to the pressure force. Therefore we will neglect this force term and first consider a simultaneous solution of the electron momentum equation with boundary conditions, only taking the pressure term into account. The validity of neglecting the Lorentz term will be verified later. The assumed electron density distribution along the electrode is plotted in Fig. 3. The radius of the plasma ball above the sheath was chosen to be about 30 μm. As we will discuss later, for this radius the calculated current density satisfies the existence criterion for a mode-0 spot, as defined in [16]. Therefore the following discussion should be considered to be valid for a mode-0 spot. Were we to have chosen to simulate a nonstationary mode-1 spot, a smaller radius would have been necessary to satisfy the corresponding existence criterion. A higher current density would then result, in better agreement with the experimental values. As the governing equations in our model are stationary, we have chosen to simulate a stationary mode-0 spot in this paper.
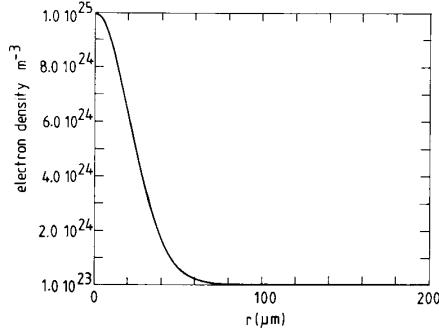
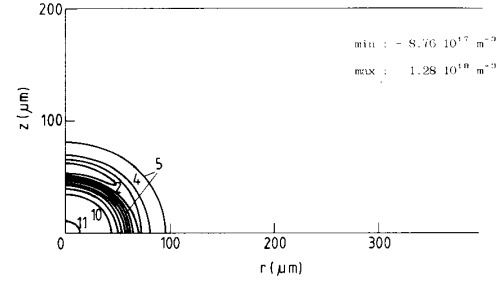Fig. 3. The electron density at the edge of the sheath.

Fig. 4. The induced-charge separation in the plasma. Numbers indicate different contour levels.
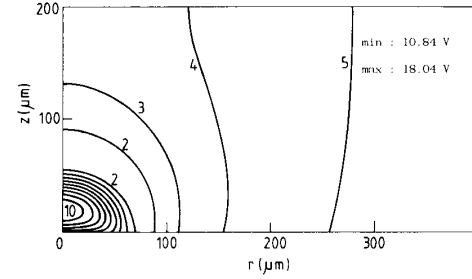

Fig. 5. The final potential distribution. Numbers indicate different contour levels.
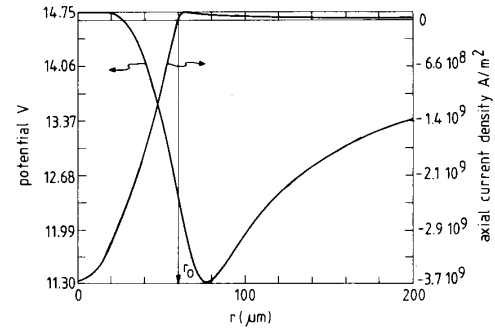

Fig. 6. The final potential and axial current density at the edge of the sheath.

The electron density profile given in Figs. 2 and 3 describes an expanding plasma. The expansion is from the origin into a low-density plasma background. The maximum density is assumed at the origin and is a hundred times as high as the background density.

Neglecting the Lorentz force, the only term in the electron momentum equation capable of inducing a charge separation is the pressure term. As we have assumed an isothermal electron gas with a constant electron density profile, this induced-charge separation does not change during iteration. This charge separation is given in Fig. 4. This figure shows that near the origin there is a depletion of electrons which are accelerated due to the pressure term towards the boundary of the expansion where a surplus of electrons arises. The charge separation calculated is much smaller than the electron density itself so that the plasma still can be considered to be quasi-neutral. As the axial component of the pressure term vanishes at the electrode, the plasma as a whole is neutral.

In the iteration process it is the boundary condition for the solution of the Poisson equation at the cathode sheath which has to be matched to the axial current density. The change in sheath potential, however, will also affect the current density, and iteration is continued. In the first step of the iteration process the potential at the cathode sheath is taken to be the floating potential. The iterative process is stopped when the current density matches the sheath potential. Then the final solution is obtained.

The final potential distribution is given in Fig. 5. The axial components of the current density and electric potential at the edge of the sheath are given in Fig. 6. In this figure r_0 represents the minimum radius for which the current density can be described by the sheath equation (1). For $r > r_0$, the current density matches the potential as given by (1). For $r < r_0$, the current density is less than $j_{sheath-min}$ and cannot be described by the sheath equation (1). There the potential difference equals the cathode fall. The radius r_0 is a calculated quantity determined in the iteration process from the current density and does not differ from the minimum radius determined in the first step. As was to be expected, r_0 equals approximately the radius of the density profile as given in Fig. 3. In Fig. 6 we also recognize the smooth transition of the potential

over the crater edge. The axial current density at the origin is about $-3.7 \ 10^9 \ \mathrm{A/m^2}$. This current density is consistent with the current density in a stationary spot at rest on a copper surface as calculated in [16].

In Fig. 7 the potential along the discharge axis is given. We see a potential hump of some 18 V in front of the sheath, and a minimum of 11 V at the edge of the expansion region. This potential distribution corresponds to a double layer just in front of the cathode surface. The implications of this potential hump on the ion motion is discussed in [17]. The calculated potential distribution can strongly affect the interpretation of the measurements to determine the cathode fall.

From the final current density distribution the current flux function can be determined. The result of this cal-
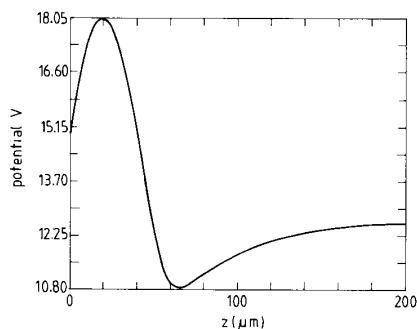
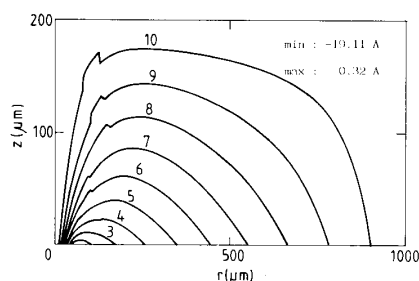Fig. 7. The electric potential along the axis of the discharge.

Fig. 8. The final current flux function. Numbers indicate different contour levels.

Fig. 9. The final azimuthal magnetic field. Numbers indicate different contour levels.

culation is given in Fig. 8. The steps in the contour lines should be considered to be artificial and can be eliminated by reducing the coarseness of the mesh. The meridional current density is parallel to the contour lines given in this figure. We clearly recognize the unipolar arc structure: For $r > r_0$ the electrode acts as the anode; for $r < r_0$, as the cathode. The calculated current is approximately 19 A and satisfies the existence condition for a mode-0 spot, as given in [16]. As the minimum sheath current density $j_{\text{sheath-min}}$ is small compared to the actual current densities, the transition from cathode to anode almost coincides with the change in sign of the normal component of the current density. This justifies the simplification that $j_{\text{sheath-min}} = 0$. Although the current distribution is influenced by the induced sheath potential, the unipolar arc structure can already be recognized in the first step of the iteration process where the sheath potential equals the floating potential all over the electrode.

From the final current density the azimuthal magnetic field can be calculated. This is the only nonvanishing component of the magnetic field and is given in Fig. 9. As for the current flux function, the steps in the contour lines are artificial. The magnetic field has a maximum of 0.07 T. The combination of this magnetic field and the meridional part of the current density causing it gives the Lorentz force. The pressure term is a factor 10 to 100 larger than the Lorentz term. Therefore the neglect of this last force component in the electron momentum equation is justified.
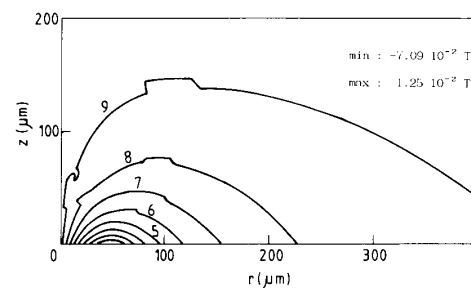
In the calculations discussed above we have assumed that the electron density and temperature profiles are given quantities. They cannot be determined from the electron momentum equation. The model calculates the electromagnetic field quantities $\underline{j}$, $\underline{E}$, and $\underline{B}$, which are consistent with the electron density and temperature profiles given.

VI. Conclusions

The aim of the calculation presented is to describe unipolar arc phenomena. The electron density profile which acts as the starting point for the calculation describes a quasi-stationary expansion of a plasma from the cathode spot on an electrode surface. For this quasi-stationary expansion the electromagnetic field quantities $\underline{j}$, $\underline{E}$, and $\underline{B}$ have been determined. The solution satisfies the electron momentum equation, Maxwell equations, and the current–voltage relation for the sheath. The most important force term in the electron momentum equation is the pressure term. The pressure-induced charge distribution has the structure of a double layer. The calculated current density is consistent with the sheath voltage. The current distribution is that of an unipolar arc: The electrode serves both as cathode and anode. The discussion given in this paper focuses on unipolar arcs.

Starting from the discussion given in this paper, the superposition of an externally applied electric field allows a description of bipolar arcs. This is the basis for the cathode spot model given in [17].

References

[1] A. E. Robson and P. C. Thoneman, "An arc maintained on an isolated metal plate exposed to a plasma," *Proc. Phys. Soc.*, vol. 73, p. 508, 1959.
[2] G. M. McCracken, "A review of the experimental evidence for arcing and sputtering in tokamaks," *J. Nucl. Mater.* vols. 93/94, p. 3, 1980.
[3] R. E. Clausing, L. C. Emerson, and L. E. Heatherly, "Arcing studies in ISX-B," *J. Nucl. Mater.*, vols. 93/94, p. 150, 1980.

[4] G. M. McCracken and D. H. J. Goodall, "The role of arcing in producing metal impurities in tokamaks," *Nucl. Fusion*, vol. 18, p. 537, 1978.

[5] S. A. Cohen, H. F. Dylla, S. M. Rossnagel, S. T. Picraux, and C. W. Magee, "Long-term changes in the surface conditions of PLT," *J. Nucl. Mater.*, vols. 76/77, p. 459, 1978.

[6] F. Schwirzke and R. J. Taylor, "Surface damage by sheath effects and unipolar arcs," *J. Nucl. Mater.*, vols. 93/94, p. 780, 1980.

[7] F. Schwirzke, in *Laser Interaction and Related Plasma Phenomena*, H. Hora and G. H. Miley, Eds. New York: Plenum, 1984, p. 335.

[8] C. Wieckert, "Plasma induced arcs," *J. Nucl. Mater.*, vols. 76/77, p. 499, 1978.

[9] E. Hantzsche, "Unipolarbögen," *Beitr. Plasmaphys.*, vol. 20, p. 329, 1980.

[10] G. Ecker, K. U. Reimann, and C. Weickert, "Electromotive force and dissipation in the plasma-induced arc," *Beitr. Plasmaphys.*, vol. 22, p. 463, 1982.

[11] D. Jütner and K. H. Krebs, "Remarks to comparing investigations about unipolar arcs in tokamaks and bipolar vacuum arcs," *Physica Scripta*, vol. 23, p. 120, 1981.

[12] V. E. Grakov, "Cathode fall of an arc discharge in a pure metal I," *Sov. Phys.—Tech. Phys.*, vol. 12, p. 286, 1967.

[13] E. Hantzsche, "Estimation of the current density in cathode arc spots," *Plasma Phys.*, vol. 25, p. 459, 1985.

[14] H. J. G. Gielen, "On the electric and magnetic field generation in expanding plasmas," Ph.D. thesis, Eindhoven Univ. of Technol., Eindhoven, The Netherlands, 1989.

[15] G. A. Mesyats, "Microexplosions on a cathode aroused by plasma–metal interaction," *J. Nucl. Mater.*, vols. 128/129, p. 618, 1984.

[16] G. Ecker, "The vacuum arc cathode: A phenomenon of many aspects," *IEEE Trans. Plasma Sci.*, vol. PS-4, p. 218, 1986.

[17] H. J. G. Gielen and D. C. Schram, "Cathode spot model," to be published.
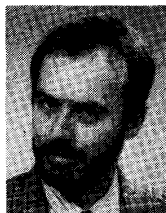
Herman J. G. Gielen was born in Eindhoven, The Netherlands, on August 30, 1960. He graduated from the Eindhoven University of Technology (Ir. degree in physics) in 1984, and received the Ph.D. degree in physics from the Eindhoven University of Technology in 1989. His Ph.D. work involved the experimental and theoretical study of the generation of electric and magnetic fields in expanding plasmas.

He joined CDL Philips Lighting B.V., Eindhoven, The Netherlands, in April 1989.

*

Daniel C. Schram was born on August 1, 1940, in Rijswijk, The Netherlands, and did his thesis work in thermonuclear fusion research on electron-cyclotron resonance.

He was involved in tokamak physics at Alcator and the FOM-laboratory. At the Eindhoven University of Technology he leads a group working on the fundamentals of plasma physics. The work includes transport phenomena, excitation, radiation, and turbulence. Also, applications such as plasma deposition are part of the program.